American Control Conference, San Diego, CA, Session TA-10, 7 June 1984

APPLICATIONS OF A NONLINEAR CONTROLLER DESIGN APPROACH BASED ON QUASILINEAR SYSTEM MODELS

James H. Taylor and Kevin L. Strobel

General Electric Corporate Research and Development
Schenectady, New York 12345

ABSTRACT

In this paper, we report on recent progress in developing nonlinear control system design techniques based on sinusoidal-input describing function (SIDF) methods. Primarily, this involves illustrating a fundamental difference between SIDF and random-input describing function (RIDF) models of nonlinear systems, developing the nonlinear controller design method more fully, and demonstrating it by applying it to a significant nonlinear control design problem in robotics. Based on these results, the use of this nonlinear controller design method should be substantially better understood.

I. INTRODUCTION

Recent research in the area of describing function methods has laid the foundation for several powerful approaches to designing controllers for nonlinear plants [1-5]. A preliminary presentation of our approach is provided in [4]; it is based on the conviction that *quasilinear* models of a nonlinear system that account for the *operating range* of system variables must provide a more realistic basis for control system design than conventional linear models. In particular, of the two basic quasilinearization or describing function methods available (random-input or RIDF, sinusoidal-input or SIDF), the *SIDF approach appears to provide the most complete characterization of the amplitude- and frequency-dependent effects of system nonlinearity.*

The SIDF method is used to develop *input/output (I/O) models* that form the basis for the systematic nonlinear control system design methodology outlined in [4]. That approach includes several methods for synthesizing linear controllers for nonlinear plants, and one method (based on inverse describing function concepts) for *synthesizing nonlinear controllers.*

The use of SIDF models as a basis for designing controllers for nonlinear plants was discussed in detail in [4]. In particular, the superiority of DF models in general in comparison with conventional linearized models based on the partial derivatives of plant nonlinearities at a specified operating point was established, and the history of certain recent developments in extending DF techniques to handle systems with multiple nonlinearities in arbitrary configurations was reviewed. Thus, we will not deal with these topics in any detail here.

The goals of this presentation are to demonstrate a fundamental difference between SIDF and RIDF models, and to show how one can use SIDF models as a basis for a systematic approach to designing nonlinear controllers for nonlinear plants. We will proceed as follows: Technical background for the SIDF approach; a single-axis robotics model; a comparison of SIDF and RIDF models of nonlinear plants; nonlinear controller synthesis for one axis of an industrial robot; and summary and conclusions.

II. THEORETICAL BACKGROUND

There are two areas that must be reviewed as the basis for the controller synthesis research presented in this paper: a definition of an SIDF-based input/output model for a nonlinear plant, and a summary of the approach for nonlinear controller synthesis [4].

II.I SIDF-based Input/Output Models for Nonlinear Plants

The basic idea of the describing function (DF) approach for studying and modeling nonlinear system behavior is to replace each system nonlinearity with a (quasi)linear term whose "gain" is a function of "input amplitude," where the form of input signal is assumed in advance. This technique is dealt with very thoroughly in a number of texts for the case of a single nonlinearity [6,7]; for systems with more than one nonlinearity in an arbitrary configuration, the most general extensions may be attributed to [8,9] in the case of random-input DFs (RIDFs) and [10-12] for sinusoidal-input DFs (SIDFs). Both of these developments have been presented in tutorial form in [13].

The SIDF approach can be used for two primary purposes: limit cycle analysis [10,11,13] and characterizing the input/output behavior of a nonlinear plant [12]. It is the latter application that serves as the basis for the research presented here. The basic equations of harmonic balance that result in such an SIDF-based I/O model for a nonlinear plant are given in [4]; in this paper, we will simply repeat the key equations necessary to define a SIDF I/O model as follows:

The nonlinear plant under consideration is characterized by the general state-variable differential equation and output equation

$$\dot{\underline{x}} = \underline{f}(\underline{x}, \underline{u}), \quad \underline{y} = \underline{h}(\underline{x}, \underline{u}) \tag{1}$$

where $\underline{x}$ is an n-dimensional state vector, $\underline{u}$ is an m-dimensional input vector, and $\underline{y}$ is a p-dimensional output

vector. We are concerned with the behavior of the plant in the presence of sinusoidal signals, so we take $\underline{u}$ and $\underline{x}$ to have the form

$$\underline{u}(t) = \underline{u}_o + \mathrm{Re}[\underline{a}\ \exp(j\omega t)],$$

$$\underline{x}(t) \cong \underline{x}_c + \mathrm{Re}[\underline{b}\ \exp(j\omega t)] \qquad (2)$$

where $\underline{u}_o$ represents the operating point or "dc value" of u(t), and $\underline{a}$ is a complex-valued vector designating the sinusoidal component amplitude and phase in the standard phasor notation. In developing SIDF models the state variables are assumed to be approximately sinusoidal, as indicated, where $\underline{b}$ is a *complex amplitude vector* and $\underline{x}_c$ is the state vector *center value*. Then we neglect higher harmonics, to approximate the right-hand sides of Eqn. (1) as follows:

$$\underline{f}(\underline{x}, \underline{u}) \cong \underline{f}_B(\underline{u}_o, \underline{a}, \underline{x}_c, \underline{b}) + \mathrm{Re}[A(\underline{u}_o, \underline{a}, \underline{x}_c, \underline{b}) \cdot \underline{b}\ \exp(j\omega t)] + \mathrm{Re}[B(\underline{u}_o, \underline{a}, \underline{x}_c, \underline{b}) \cdot \underline{a}\ \exp(j\omega t)] \qquad (3)$$

$$\underline{h}(\underline{x}, \underline{u}) \cong \underline{h}_B(\underline{u}_o, \underline{a}, \underline{x}_c, \underline{b}) + \mathrm{Re}[C(\underline{u}_o, \underline{a}, \underline{x}_c, \underline{b}) \cdot \underline{b}\ \exp(j\omega t)] + \mathrm{Re}[D(\underline{u}_o, \underline{a}, \underline{x}_c, \underline{b}) \cdot \underline{a}\ \exp(j\omega t)]$$

Minimum mean square approximation error is obtained when the real vectors $\underline{f}_B$ and $\underline{h}_B$ and the matrix set {A, B, C, D} are obtained by taking the first two terms of the Fourier expansions of the elements of $\underline{f}(\underline{x}, \underline{u})$ and $\underline{h}(\underline{x}, \underline{u})$ with $\underline{x}$, $\underline{u}$ of the form indicated in Eqn. (2). This approach has been discussed and illustrated in detail in [6,7,13]. The DF arrays $\{\underline{f}_B, \underline{h}_B\}$ and {A, B, C, D} in Eqn. (3) provide the quasilinear representation of the nonlinear plant in Eqn. (1) for a particular amplitude and frequency; the constant or d.c. portion of the model is described by $\underline{f}_B$ and $\underline{h}_B$, while the matrix set {A, B, C, D}, which conforms to the usual linearized model notation, characterizes the plant response to sinusoidal inputs. The two signal components (d.c., first harmonic) are coupled, as the above notation suggests, due to the failure of superposition in nonlinear systems. Setting up the SIDF arrays in Eqn. (3) in analytic form is often a simple matter: A wide variety of SIDFs for single-input nonlinearities have been catalogued [6,7], and handling multi-input nonlinearities has been dealt with in some detail in [10,13].

Using SIDFs to determine the approximate response of a nonlinear plant to sinusoidal inputs is treated in [6,7] in the case of systems with a single nonlinearity, and was extended to the multiple nonlinearity case in a modern algebraic setting in [12]. Applying the conditions of harmonic balance to the quasilinear model given in Eqn. (3) leads to a set of nonlinear algebraic equations that can be solved to obtain $\{\underline{x}_c, \underline{b}\}$ as determined by $\{\underline{u}_o, \underline{a}\}$ as follows:

$$\underline{f}_B(\underline{u}_o, \underline{a}, \underline{x}_c, \underline{b}) = \underline{0},$$

$$\underline{b} = [j\omega I - A(\underline{u}_o, \underline{a}, \underline{x}_c, \underline{b})]^{-1} B(\underline{u}_o, \underline{a}, \underline{x}_c, \underline{b})\ \underline{a} \qquad (4)$$

These 2n nonlinear algebraic equations (n of which are complex-valued) can be solved readily using standard computer routines; for example, MINPACK [14] has proven to be an excellent package for this application. In this case, one should be careful to ensure that A does not have eigenvalues on or very close to the imaginary axis; otherwise limit cycles may exist in addition to the response to the sinusoidal input, in contradiction to the assumptions underlying Eqns. (2,3).

The sinusoidal component of the plant response can then be characterized by the input-amplitude-dependent matrix "transfer function"

$$G(j\omega; \underline{u}_o, \underline{a}) = C(j\omega I - A)^{-1} B + D \qquad (5)$$

where the SIDF matrices are explicitly determined by $\{\underline{u}_o, \underline{a}\}$, since $\{\underline{x}_c, \underline{b}\}$ are eliminated using Eqn. (4). To simplify notation, in cases where the operating point $\underline{u}_o$ is zero, the I/O relation will be denoted $G(j\omega; \underline{a})$.

This modern algebraic method for determining the "frequency response" (Eqn. (5)) for a nonlinear plant serves as one basis for nonlinear controller design. Observe that the DF arrays vary with frequency, so that it is not possible to work with {A, B, C, D} in any other sense than in Eqn. (5). In particular, it is not clear what significance might be ascribed to the eigenvalues of A at any particular frequency, except possibly to view their amplitude dependence as a measure of the impact of nonlinearity on the behavior of the system.

There is another, more direct way to obtain an SIDF-like amplitude-sensitive plant model: *Simulation plus fourier transform methods* [3]. This approach is well known for single-input single-output plants; it has recently been extended to the multi-input multi-output case [15]. Using either approach, the designer can obtain the required SIDF model in a straightforward manner. Thus, we will not consider the computational aspects of the SIDF approach further.

II.II Designing Nonlinear Controllers

The following approach, which has been called the *inverse DF synthesis method* [4] should prove to be effective in many situations where it is necessary to obtain high performance from plants with a substantial degree of nonlinearity:

1. Choose a *number of design ranges* as defined by $\{\underline{u}_o, \underline{a}\}$ in Eqn. (2) and obtain a SIDF I/O model for each range.
2. Select a *fixed controller configuration* (e.g., PID, lead, lag-lead, etc.).
3. Design a controller of the selected type *for each SIDF model* (controllers must be based on the same specifictions; some or all controller parameters will differ for different design ranges).
4. Interpret the amplitude-dependent controller parameters as *describing functions* for controller nonlinearities; invert the SIDF's to obtain the corresponding nonlinear element.
5. Validate the nonlinear control system design by simulation.

A conceptual illustration of this approach and a discussion of several ways one might carry out the SIDF inversion process needed for the fourth step were provided in [4].

The justification for this design technique is simply that a nonlinear controller is much more likely to provide the desired performance over a wide range of operation than a linear one if the basic input/output behavior of the plant (as characterized by the various SIDF I/O models) differs substantially. These models serve as a primary way of determin-

ing whether or not there is a potential payoff in the use of a nonlinear controller, and in developing it. This will be illustrated in the application in Section 5.

III. A SINGLE-AXIS ROBOTIC ARM MODEL

In this section, we provide a differential equation set describing the behavior of a single-axis robotic arm. In addition, we outline how realistic parameter values were obtained for a specific robot of interest, and summarize how the importance of the various nonlinear effects was determined in order to simplify analysis and design.

III.I Dynamic Equations of Motion

The model presented here describes a single-axis position servo for an industrial robotic arm. The form of this model is characteristic of a revolute robot (one that contains only rotational joints). Dynamic coupling effects between axes are modeled as load torque disturbances, thereby reducing the system to a motor driving a load through compliant gearing. Over the frequency band of interest the load can be modeled by a lumped mass, yielding the two-mass dynamic model shown in Fig. 1.

The motor is acted upon by viscous friction, $f_{Mv}(\omega_M) = B_M\,\omega_M$, and coulombic friction, $f_{Mc}(\omega_M) = C_M\,sign(\omega_M)$. The load damping is similar in form, as indicated in the figure. The motor and load are connected by a nonlinear (hardening) spring, $f_{Rk}(\theta_L - \theta_M)$, which also contains relative viscous damping f_{Rv}. A DC servo motor driven by pulse width modulation and a current loop has electrical dynamics fast enough to assume constant voltage command to armature current (I_c / e_i) and armature current to motor torque (T_M / I_c) transfer functions over the necessary frequency range. Thus, the differential equations and transfer functions defining the relationships among voltage command and motor and load velocity and position are given as follows:

$$\dot{\omega}_M = -\,[(f_{Mv} + f_{Mc}(\omega_M) + f_{Rv})\,\omega_M - f_{Rv}\,\omega_L + f_{Rk}(\theta_M - \theta_L)\cdot(\theta_M - \theta_L) - K_v e_i]/J_M$$

$$\dot{\theta}_M = \omega_M \tag{6}$$

$$\dot{\omega}_L = -\,[(f_{Lv} + f_{Lc}(\omega_L) + f_{Rv})\,\omega_L - f_{Rv}\,\omega_M - f_{Rk}(\theta_M - \theta_L)\cdot(\theta_M - \theta_L)]/J_L$$

$$\dot{\theta}_L = \omega_L$$

where all symbols are defined in Fig. 1. With the following definitions of linearized coefficients,

$$B_M \cong f_{Mv} + f_{Mc}(\omega_M), \quad B_L \cong f_{Lv} + f_{Lc}(\omega_L)$$

$$B_R = f_{Rv}, \qquad K \cong f_{Rk}(\theta_M - \theta_L) \tag{7}$$

we can write the transfer function relations as:

$$\omega_M/e_i\,(s) = [K_v(J_L s^2 + (B_L + B_R)s + K)]/D(s)$$

$$\omega_L/e_i\,(s) = [K_v(B_R s + K)]/D(s) \tag{8}$$

where

$$D(s) = J_M J_L s^3 + [J_M(B_L+B_R) + J_L(B_M+B_R)]s^2 + [K(J_M+J_L) + B_M B_L + B_R(B_M+B_L)]s + K(B_M+B_L)$$

The servo system shown in Fig. 2 is used to control load position θ_L. The two inner loops feed back motor velocity ω_M and motor position θ_M to give a fast, well-damped motor response for signals small enough not to cause excessive saturation. The objective is to design a nonlinear PID load position error compensator to give the best possible performance for small, medium and large input signals.

III.II Identifying Nonlinear Models

Because of its insensitivity to gravity loading and therefore ease of experimental measurement, the base rotation axis of a GE P50 robot was chosen for parameter identification.

In the case of linear systems, it is a common practice to derive model parameters by measuring the frequency response experimentally, fitting a transfer function in ratio-of-polynomial form to the data, and solving for the system parameters corresponding to the polynomial coefficients. With some modification this method can be adapted for use on nonlinear systems as well [16].

Briefly, identification of nonlinear system parameters in the frequency domain is performed as follows: Determine constant input amplitude frequency responses $G(j\omega; \underline{a})$ as in Eqn. (5) for several amplitudes. Fit an equivalent linear model, in the form of a ratio of polynomials transfer function, to each $G(j\omega; \underline{a})$. Using a physically-defined mathematical model such as the one described above (Eqns. (6-8)), find equivalent linear system parameters by equating polynomial coefficients and solving the equations thus obtained. Simulate each equivalent linear system and obtain amplitudes for the inputs to each nonlinearity. Then, by viewing the parameter variations among the various linear models as describing function values and, knowing the input amplitudes to the nonlinearities from the last step, these SIDF's may be inverted to get parameters for the nonlinear model. This method was applied to the GE P50 industrial process robot and yielded good agreement between measured parameters and specifications published by the component manufacturers. A more detailed discussion of this approach may be found in [16].

III.III Important Nonlinear Effects

To facilitate simulation, analysis and design, it is desirable to remove unimportant nonlinearities from the model and replace them by equivalent linearized terms based on the behavior of the system for medium input amplitudes. In the system defined above, it has been determined that not all of the nonlinearities are important when designing a load position controller. This is intuitively reasonable, since experience indicates that closing a tight velocity loop around a motor increases effective motor damping, thereby significantly reducing the effects on system performance caused by nonlinear motor characteristics and load coupling. With this in mind, variations in the performance of the open load-position loop (the forward path in Fig. 2 with both the motor velocity and position loops closed) were investigated for various signal amplitudes. It was thereby shown that the most significant nonlinear effect is the limitation on the amount of torque available for control.

To justify this simplification, it is necessary to perform comparative simulations so that the system can be shown to be realistically modeled by the resulting more linear model. First, we compared simulated step responses for three cases: the first case was the response of the equivalent linear model; the second and third cases were time histories obtained using the nonlinear model with small and large step inputs. This showed that the nonlinearities in question could be replaced by equivalent linear terms without sacrificing appreciable accuracy. Also, since controller design is being done with frequency domain methods, we compared $G(j\omega; \underline{a})$ under appropriate conditions. Using the fully nonlinear and partially linearized models showed that the SIDF I/O relations are similar enough to justify designing with a more linear model. This comparison is portrayed in Fig. 3.

As a result of this process, parameters for the partially linearized model are as follows:

$$J_M = 2.8\times10^{-3}\ kg-m^2, \qquad J_L = 1.2\times10^{-3}\ kg-m^2,$$

$$K = 5.4 Nm/rad, \qquad K_v = 1.2 Nm/v, \tag{9}$$

$$B_M = 3.9\times10^{-2}\ Nm-s/rad, \quad B_L = 1.0\times10^{-3}\ Nm-s/rad,$$

$$B_R = 6.4\times10^{-3}\ Nm-s/rad$$

IV. SIDF AND RIDF MODELS

It is well-known [6,7] that there are two conceptual differences between SIDF and RIDF models for a nonlinearity: The assumed input amplitude distribution is different, and SIDFs can characterize the effective "phase shift" caused by multivalued nonlinearities such as those commonly used to represent hysteresis and backlash, while RIDFs cannot. These issues were both discussed in some detail [4]; in particular, it was shown that the input amplitude distribution issue is generally not a major consideration. The importance of the "effective phase shift" issue appears to be a matter of modeling judgment; it may be argued that hysteresis and backlash can be modeled without the use of multivalued nonlinearties, which would negate the second difference in choosing which DF method to employ.

However, there is a third difference (observed earlier in [17]) that impacts the *I/O model of a nonlinear plant* in a much more substantive way. This difference is unrelated to the form of the DF gain as a function of amplitude, but rather, is based on how the DF is used in determining the I/O model. The result is that the RIDF plant model (as it is usually defined [2,4]) is not as informative as the SIDF one in terms of capturing the frequency dependence of the system nonlinear effects.

This difference arises from the fact that the standard RIDF model is the result of *one* quasilinearization procedure carried out over a wide band of frequencies, while the SIDF model is obtained by quasilinearizing at a *number* of frequencies. This difference is best understood via the simple example presented below; we will also demonstrate that it is a significant issue in the robotic control problem that is the major focus of the paper.

IV.I A Simple Example: Low Pass Dynamics with Saturation

The frequency dependence of a nonlinear effect can be seen by a simple example proposed in [17] involving a low-pass linear system followed by a unity saturation, Fig. 4. Considering sinusoidal inputs of suitably chosen amplitude, the following behavior is exhibited: Low frequency inputs are only slightly attenuated by the linear dynamics, resulting in large saturation effects. However, as frequency increases, the attenuation also increases, and saturation correspondingly decreases and eventually disappears, giving a response that approaches the output of the low-pass linear dynamics alone. A random input, on the other hand, results in a frequency response plot that is identical to the linear dynamics followed by a gain less than unity. To demonstrate this, the system of Fig. 4 was analyzed and Bode plots were obtained using standard linearization and the SIDF and RIDF approaches. The input amplitude 3.0 was chosen for the sinusoidal analysis, and the RIDF frequency response was derived assuming that the system was driven by a gaussian white noise process with a spectral density such that the standard deviation at the input to the saturation had the same rms value as the sinusoid at low frequency (3.0*0.707). These results are also portrayed in Fig. 4. For design purposes, the SIDF approach captures both a gain change and an effective increase in the transfer function magnitude corner frequency, while the RIDF model shows only a gain reduction.

IV.II SIDF and RIDF Models for the Robotic Arm Model

The phenomenon depicted in Fig. 4 is also important in the robotics problem under study. Figure 5 shows the similarities between experimental and simulation-derived random input frequency data, and the differences between SIDF and RIDF frequency responses. It is evident that the differences between these two DF models is substantial, especially at low frequencies and in the vicinity of the lightly-damped pole/zero pairs at about 70 radians per second.

The simple example above explains why RIDF and SIDF differ and why the SIDF information is more meaningful. Figure 5 shows that this is important in a real-world problem. This difference could be reduced by using RIDF analysis based on an ensemble of narrow-band random inputs to obtain the frequency dependence of the I/O relation. In the limit as more narrow-band noise inputs are considered, one approaches the SIDF I/O model, except for the fact that the amplitude distribution is different. In so doing, it would be necessary to design controllers in the frequency domain rather than in the time domain, since one would no longer obtain a single {A, B, C, D} set that could be used in conjunction with the LQG approach as has been done in the past [1,2,5]. It would be interesting to see what advantages could be obtained using an intermediate case; to the best of our knowledge, this approach has not been carried out.

V. NONLINEAR CONTROLLER SYNTHESIS

We will now illustrate how SIDF methods can be used to synthesize nonlinear controllers that provide better performance than can be obtained using linear methods and which are difficult or impossible to obtain using intuition.

V.I SIDF Design of a Stabilizing Nonlinear Gain

The first step in controller design for a nonlinear plant is the determination that the effect of nonlinearity is indeed substantial enough to require a nonlinear controller. The best measure of the importance of nonlinearity in the context of our approach for controller design is the variability of the SIDF I/O model for a number of input amplitudes that

characterizes "typical" operating regimes of the plant. This determination was done in an indirect way, as follows: A PID controller was designed to provide good performance for small inputs (commanded input of 50 millivolts); a polar plot of the compensator and plant is shown in Fig. 6. Then the Fourier-analysis based approach was used to generate $C(j\omega)\cdot G(j\omega; a)$ for a number of values of a where a is the amplitude of the input to the compensator: a = 200, 400, 800, and 1600 mv, as portrayed in Fig. 7. These results are completely consistent with our findings that the closed-loop system designed on the basis of small signals is unstable for medium and large step inputs.

The polar plots in Fig. 7 show that the closed-loop system can be stabilized by reducing the gain by at least 50 percent; this result is also consistent with step response simulations. However, it would be desirable to retain the faster response for small signals. The inverse SIDF synthesis approach (Section 2.2) can be used to accomplish this objective. The specific steps we used are as follows:

1. Draw scaled M-circles for reduced open-loop gain values, as shown in Fig. 8.
2. Obtain values of K(a) that result in the polar plot for each value of a being tangential to the corresponding M-circle.
3. Synthesize a piece-wise linear characteristic whose SIDF fits the K(a) relationship, Fig. 9.

The outcome of this design approach is a nonlinear controller that provides a large-signal performance that is comparable to that of the reduced-gain linear controller that achieves stable response for all input amplitudes (K = 0.5), while maintaining a faster response for small step inputs (Fig. 10).

V.II SIDF Design of a Fully Nonlinear PID Controller

We then considered the possible advantages of using a fully nonlinear PID controller, i.e., one having a nonlinearity in each term (P, I, D) in the compensator as proposed in [4]. The benefit of such a controller in comparison with a single nonlinear gain as designed above is clearly that there are more degrees of freedom that may be used to obtain better or less amplitude-dependent behavior; it is also clear that these benefits will be advantageous only if the $G(j\omega; a)$ plots are *substantially different in their frequency dependence.* In other words, if the Bode plots of $G(j\omega; a)$ differ primarily in terms of a gain shift, then the extra degrees of freedom will not have significant payoff in terms of improved performance.

For the problem at hand, the family of Bode plots portrayed in Fig. 11 for the input amplitudes considered does not seem to show the required differences in frequency response, so we have not attempted to design a fully nonlinear PID in light of the judgement that the performance improvement would be too insignificant to be worth the trouble.

VI. SUMMARY AND CONCLUSIONS

The modern algebraic formulation of the sinusoidal-input describing function method for modeling and analyzing nonlinear systems brings this approach to such a state of power, generality, and analytic simplicity that we believe it will come to play a major role in nonlinear systems design. This statement was argued conceptually in some detail in [4]; the main contributions of this paper are the clarification of a major difference between SIDF and RIDF input/output models of nonlinear plants, and the elucidation of some implementation issues (significance of $G(j\omega; a)$; making the forward path as amplitude insensitive as possible) and the potential performance advantages that may be possible using these techniques. It is hoped that this design approach will provide a framework for further developments in the realm of controller design for nonlinear systems.

REFERENCES

[1] Rajarao, B. V. and Mahalanabis, A. K., "On Optimization of Nonlinear Stochastic Systems," *Internat. J. of Control*, Vol. 11, pp. 561 - 570, April 1970.

[2] Hedrick, J. K., "The Use of Statistical Describing Functions with Linear-Quadratic-Gaussian Controller Design," *Proc. Joint Auto. Control Conf.*, West Lafayette, IN, pp. 390-393, 1976.

[3] Taylor, J. H., "Robust Computer-Aided Control System Design for Nonlinear Plants," Application of Multivariable Systems Theory, Manadon, Plymouth, UK, October 1982.

[4] Taylor, J. H., "A Systematic Nonlinear Controller Design Method Based on Quasilinear System Models," *Proc. American Control Conf.*, San Francisco, CA, pp. 141-145, 1983.

[5] Beaman, J. B., "Application of Statistical Linearization and LQG Design to Position Control," *Proc. American Control Conf.*, San Francisco, CA, pp. 127-131, 1983.

[6] Atherton, D. P., *Nonlinear Control Engineering*, Van Nostrand Reinhold, London, 1975 (Student Edition, paperback, 1982).

[7] Gelb, A. and Vander Velde, W. E., *Multiple-Input Describing functions and Nonlinear System Design*, McGraw-Hill, New York, 1968.

[8] Kazakov, I. E., "Generalization of the Method of Statistical Linearization to Multi-Dimensional Systems," *Avtomatika i Telemekhanica*, Vol. 26, 1210-1215, 1965.

[9] Gelb, A. and Warren, R. S., "Direct Statistical Analysis of Nonlinear Systems: CADET," *AIAA J.*, Vol. 11, 689-694, 1973.

[10] Taylor, J. H., "An Algorithmic State-Space/Describing Function Technique for Limit Cycle Analysis," TIM-612-1, The Analytic Sciences Corp. (TASC), Reading, MA, 1975.

[11] Hannebrink, D. N., Lee, H. S. H., Weinstock, H. and Hedrick, J. K., "Influence of Axle Load, Track Gauge, and Wheel Profile on Rail Vehicle Hunting," *Trans. ASME - J. Eng. Ind.*, 186-195, 1977.

[12] Taylor, J. H., "Describing Function Methods for High-Order Highly Nonlinear Systems," *Proc. Intl. Cong. on Appl. Systems Research and Cybernetics*, Acapulco, Mexico, 1980.

[13] Ramnath, R. V., Hedrick, J. K., and Paynter, H. M. (editors) *Nonlinear System Analysis and Synthesis: Volume 2 - Techniques and Applications*, American Society of Mechanical Engineers, Book G00178, 1980. See particularly chapters 7, 9, 13, 16.

[14] More, J. J., Garbow, B. S. and Hillstrom, K. E., "User Guide for MINPACK-1," Argonne National Laboratory Report No. ANL-80-74, August, 1980.

[15] Taylor, J. H., "Computer-Aided Control Engineering Environment for Nonlinear Systems," submitted to the Third IFAC Symposium *CAD in Control and Engineering Systems*, The Technical University of Denmark, Lyngby, Denmark, August 1985.

[16] Strobel, K. L., "Describing Function Methods with Applications to Robotics," Master's Project Report, Rensselaer Polytechnic Institute, May, 1984.

[17] Taylor, J. H., "A Systematic Nonlinear Controller Design Method Based on Quasilinear System Models," General Electric Corporate Research and Development Report No. 83CRD139, June 1983 (a slightly expanded version of [4]).

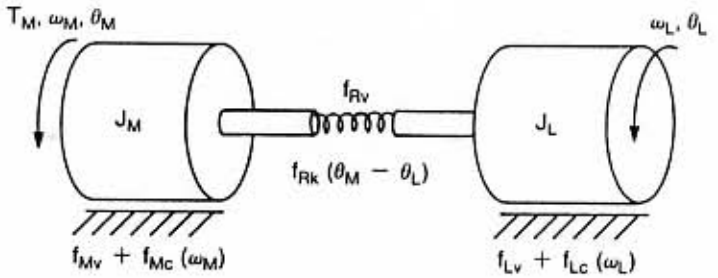

Figure 1. Single-Axis Robot Model Schematic

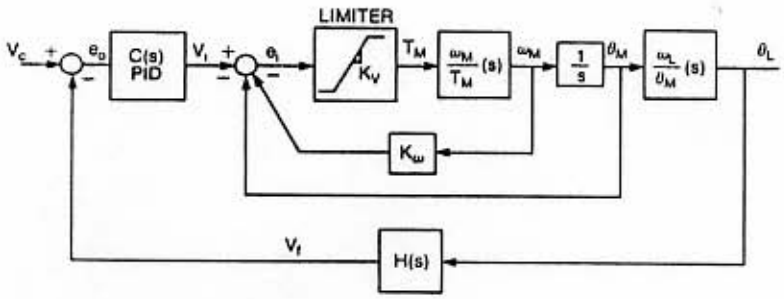

Figure 2. Robotic Position Control Servomechanism

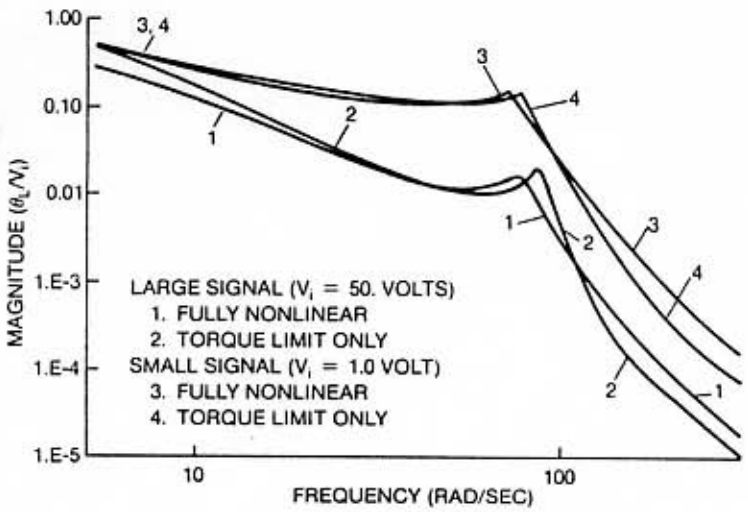

Figure 3. Validation of Partially Linearized Model

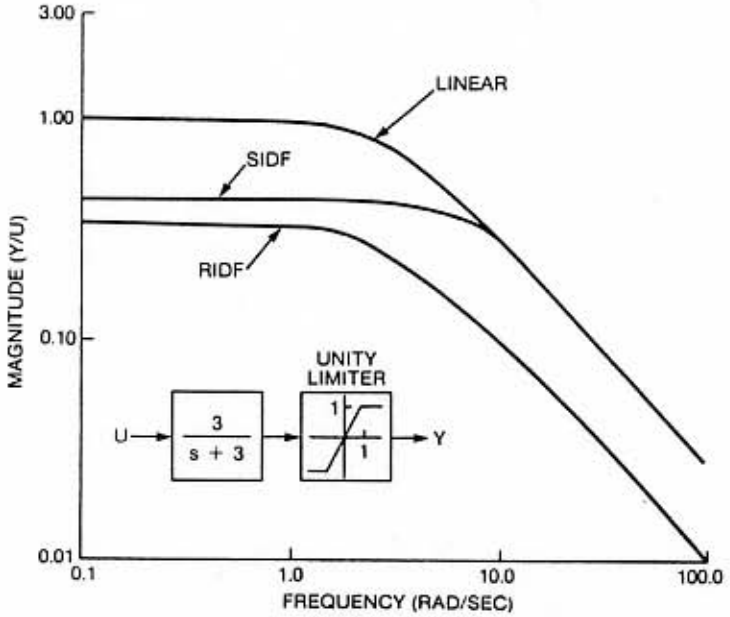

Figure 4. Simple Comparison of RIDF and SIDF Models

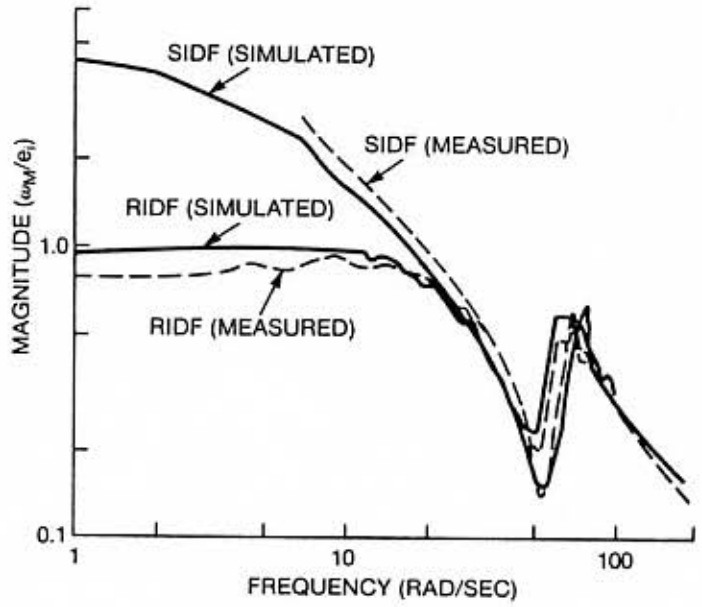

Figure 5. Comparison of RIDF and SIDF Robotics Models

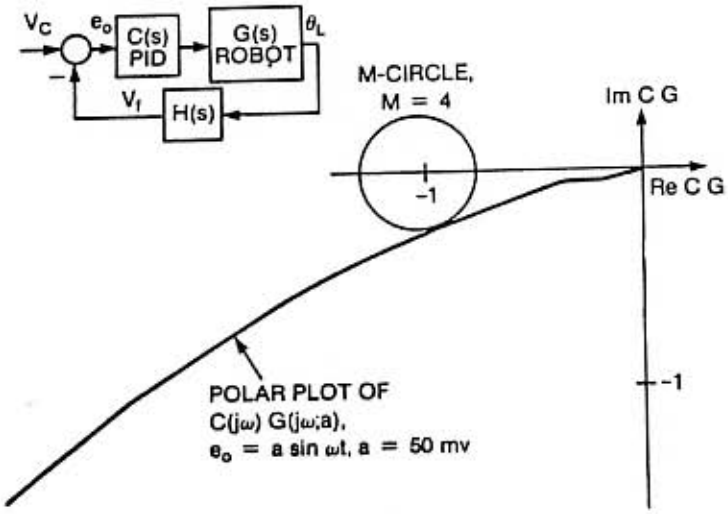

Figure 6. PID Controller Design for Small Signals

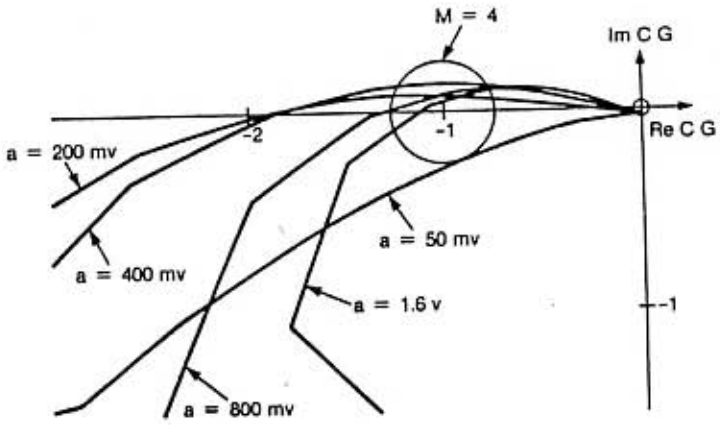

Figure 7. Polar Plots Showing Instability Due to Torque Limits

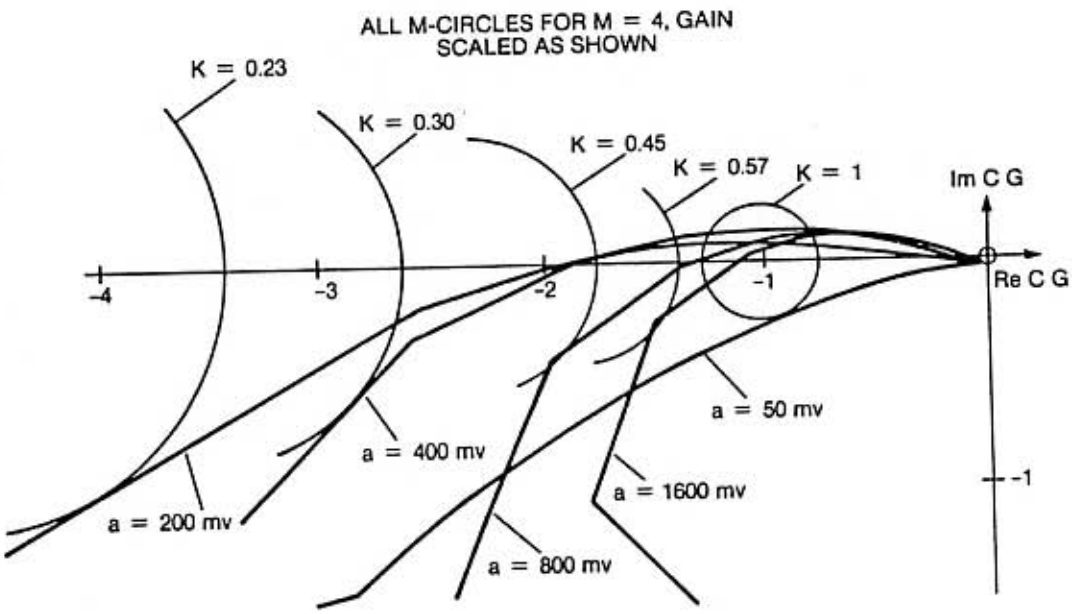

Figure 8. Obtaining Amplitude-Dependent Gain Via M-Circles

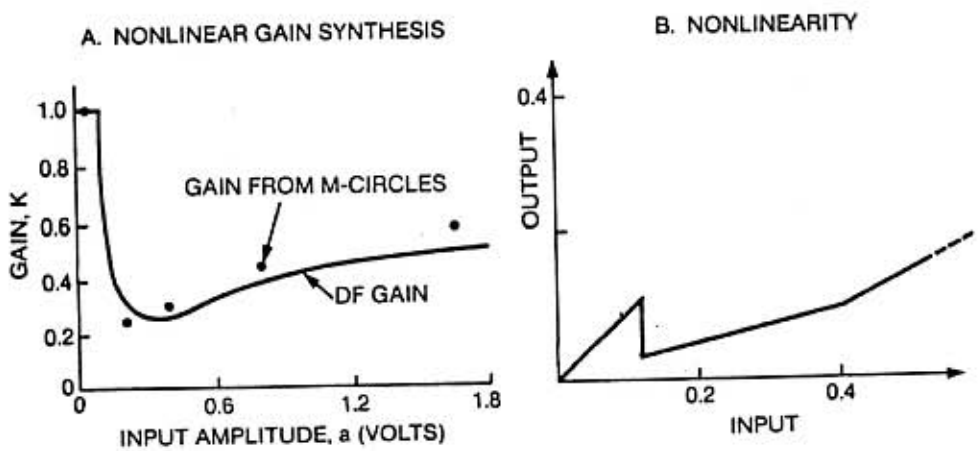

Figure 9. SIDF Inversion to Synthesize the Nonlinear Controller

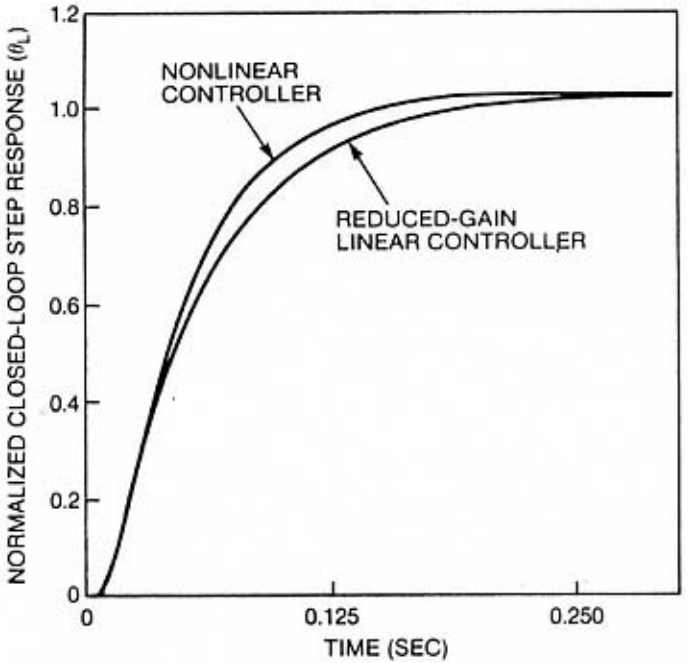

Figure 10. Linear and Nonlinear Performance Comparison for Small Signals

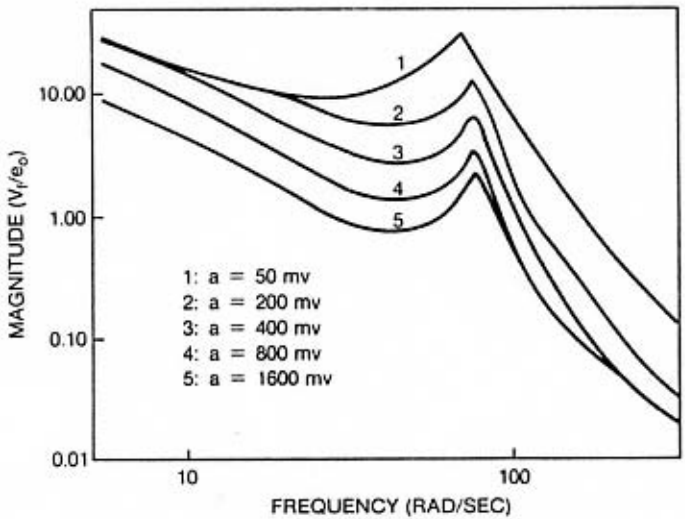

Figure 11. Amplitude-Dependent $C \cdot G \cdot H(j\omega)$ Magnitude Plots